

# Analyst

Accepted Manuscript



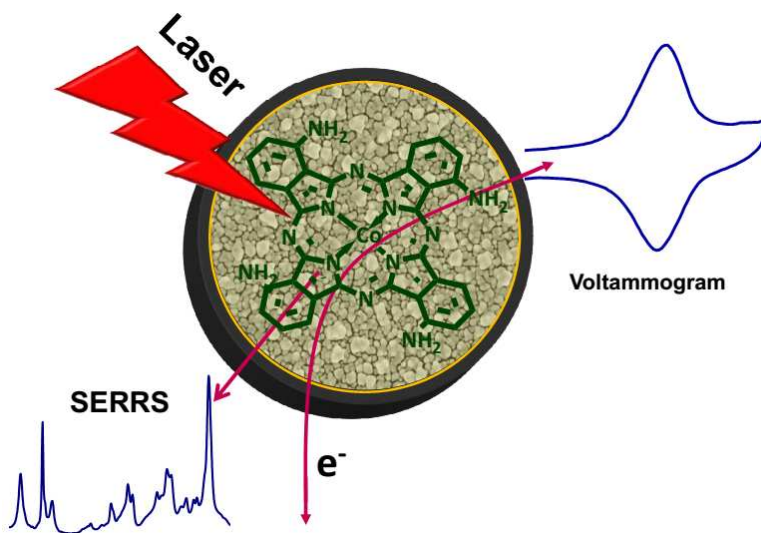
This is an *Accepted Manuscript*, which has been through the Royal Society of Chemistry peer review process and has been accepted for publication.

*Accepted Manuscripts* are published online shortly after acceptance, before technical editing, formatting and proof reading. Using this free service, authors can make their results available to the community, in citable form, before we publish the edited article. We will replace this *Accepted Manuscript* with the edited and formatted *Advance Article* as soon as it is available.

You can find more information about *Accepted Manuscripts* in the [Information for Authors](#).

Please note that technical editing may introduce minor changes to the text and/or graphics, which may alter content. The journal's standard [Terms & Conditions](#) and the [Ethical guidelines](#) still apply. In no event shall the Royal Society of Chemistry be held responsible for any errors or omissions in this *Accepted Manuscript* or any consequences arising from the use of any information it contains.

Graphical Abstract



1  
2  
3  
4  
5  
6  
7  
8  
9  
10  
11  
12  
13  
14  
15  
16  
17  
18  
19  
20  
21  
22  
23  
24  
25  
26  
27  
28  
29  
30  
31  
32  
33  
34  
35  
36  
37  
38  
39  
40  
41  
42  
43  
44  
45  
46  
47  
48  
49  
50  
51  
52  
53  
54  
55  
56  
57  
58  
59  
60

## Towards improved precision in the Quantification of Surface-Enhanced Raman Scattering Enhancement Factor: A Renewed Approach

Arumugam Sivanesan,<sup>\*ab</sup> Witold Adamkiewicz,<sup>a</sup> Govindasamy Kalaivani,<sup>b</sup> Agnieszka Kamińska,<sup>\*a</sup> Jacek Waluk,<sup>a</sup> Robert Hołyst<sup>a</sup> and Emad L. Izake<sup>b</sup>

<sup>a</sup>*Institute of Physical Chemistry, Polish Academy of Sciences, Kasprzaka 44/52, 01-224 Warsaw, Poland*

<sup>b</sup>*Nanotechnology and Molecular Sciences Discipline, Faculty of Science and Engineering, Queensland University of Technology, 2 George St., Brisbane, QLD 4001, Australia.*

\* Corresponding authors:

E-mail address: [asnesan@gmail.com](mailto:asnesan@gmail.com); [sivanesan.arumugam@qut.edu.au](mailto:sivanesan.arumugam@qut.edu.au) (A. Sivanesan) Tel: +61 07 3138 0607

E-mail address: [akamin@ichf.edu.pl](mailto:akamin@ichf.edu.pl) (A. Kamińska) Tel: +48 22 343 32 28

**Abstract**

This paper demonstrates a renewed procedure for the quantification of surface-enhanced Raman scattering (SERS) enhancement factor with improved precision. The principle of this method relies on deducting the resonance Raman scattering (RRS) contribution from surface-enhanced resonance Raman scattering (SERRS) to end up with surface enhancement (SERS) effect alone. We employed 1,8,15,22-tetraaminophthalocyanato-cobalt(II) ( $4\alpha\text{-Co}^{\text{II}}\text{TAPc}$ ), a resonance Raman- and electrochemically redox- active chromophore, as a probe molecule for RRS and SERRS experiments. The number of  $4\alpha\text{-Co}^{\text{II}}\text{TAPc}$  molecules contributing to RRS and SERRS phenomenon on a plasmon inactive glassy carbon (GC) and plasmon active GC/Au surfaces, respectively have been precisely estimated by cyclic voltammetry experiments. Furthermore, the SERS substrate enhancement factor (SSEF) quantified by our approach is compared with the traditionally employed methods. We also demonstrate that the present approach of SSEF quantification can be applied for any kind different SERS substrate by choosing an appropriate laser line and probe molecule.

**Keywords:** Surface-enhanced Raman scattering (SERS), voltammetry, nanostructure, SERS substrate enhancement factor (SSEF), quantification of SERS enhancement factor, 1,8,15,22-tetraaminophthalocyanato- cobalt(II).

## 1. Introduction

Surface-enhanced Raman spectroscopy (SERS) was discovered 40 years ago<sup>1</sup> and nowadays it is becoming one of the most popular ultrasensitive analytical techniques.<sup>2, 3</sup> Recently, highly sensitive analyses, even at a single molecule level, were achieved with SERS,<sup>4-6</sup> which widened the analytical potential and versatility of this technique. Undoubtedly, the most important issue regarding SERS effect is the precise quantification of substrate enhancement factor (SSEF) (i.e., the magnitude of the enhancement). A criticism often underlined is that SERS is still not transferred into practical analytical applications. This is linked with difficulties in measuring the SSEF rigorously. Careful experimental quantification of SSEF is particularly crucial while designing a useful analytical tool based SERS. The enhancement factor is also an important figure for characterization of SERS substrates. Although wide varieties of SERS substrates have been produced for the last four decades, there is no standard procedure to assess the quality of the SERS substrate. i.e., the issue of precise quantification of SERS substrate enhancement factor has not been solved until now. The materials chemists involved in the preparation of substrates always face the major problem in sorting out their best SERS substrate. Therefore, also from the materials science point of view, the precise quantification of SSEF is essential. The questions of the magnitude of the enhancement and the origin of the SERS enhancement are again in the spotlight of researchers, together with those regarding the uncertainty and the interpretation of the pioneering single-molecule (SM) SERS study.<sup>7, 8</sup> There are still conflicting viewpoints in SM-SERS, including interpretation of nature and magnitude of the enhancement. Several papers focused on the presentation and discussion of experimental quantification of the enhancement factor.<sup>9-14</sup> However, the reported methods have shortcomings

1  
2  
3 in their approach and methodology. For example, the most widely used equation for the  
4  
5 estimation of SSEF is:<sup>12-14</sup>  
6  
7

$$8 \quad \text{SSEF} = \frac{I_{\text{SERS}} \cdot N_{\text{Vol}}}{I_{\text{RS}} \cdot N_{\text{Surf}}} \quad (1)$$

9  
10  
11  
12  
13 Where  $N_{\text{Vol}} = c_{\text{RS}}V$  is the average number of molecules in the scattering volume ( $V$ ) for the  
14  
15 Raman (non-SERS) measurement, and  $N_{\text{Surf}}$  is the average number of adsorbed molecules in the  
16  
17 scattering volume of the SERS experiments. The above definition presents a few challenges to  
18  
19 the accurate quantification of the SERS effect.<sup>15, 16</sup>  
20  
21  
22  
23

24 Arguably, the molecules (Rhodamine 6G, 4-aminothiophenol, p-mercaptobenzoic acid,  
25  
26 etc.) which are supposed to be standard objects for the quantification of SSEF cause difficulty in  
27  
28 estimating the Raman cross-section both in solution and also on surface. Actually, the dye  
29  
30 molecules have larger Raman cross-sections up to  $10^5 - 10^6$  in resonant<sup>17</sup> and pre-resonant  
31  
32 conditions which are not considered in the estimation of Raman cross-section. In other words,  
33  
34 the calculation of Raman cross-section by density functional theory assumes a non-resonant  
35  
36 condition which is suitable for normal Raman spectra. Therefore, the values calculated using this  
37  
38 approach will not be applicable even under pre-resonant conditions<sup>18</sup> and hence an alternative  
39  
40 approach or method is required. Furthermore, the Raman cross-section may also depend on the  
41  
42 effect of the substituents in the probe molecule and also on other factors, that are not considered  
43  
44 in the existing quantification equations, such as the interaction with solvent molecules. It is  
45  
46 worth mentioning here that the  $I_{\text{Raman}}$  depends on the refractive index of the solvent. Limitations  
47  
48 also exist in calculating  $N_{\text{Surf}}$  as the number of the probe molecules on the surface is estimated by  
49  
50 assuming an ideal Langmuir monolayer. In reality, it is hard to achieve defect-free monolayer.  
51  
52  
53  
54  
55  
56  
57  
58  
59  
60

1  
2  
3 Instead a multilayer of the probe molecule (e.g., 4-aminothiophenol) may exist on the SERS  
4 substrate and would result in incorrect estimation of  $N_{\text{Surf}}$ . Moreover, estimating surface  
5 scattering volume is not rigorous in many cases, as it is difficult to determine the exact active  
6 surface area of the substrate. There is also an inconsistency in rigorous quantification of  
7 parameters such as effective scattering volume and scattering area in solution. Because of these  
8 challenges surrounding the optimization and control of experimental parameters in SERS  
9 experiments may be one of the reasons for the unusually high SSEF, up to  $10^{14}$ , that are reported  
10 in literature.<sup>16, 17</sup>

11  
12  
13 Recently, Le Ru and coworkers attempted to address these issues by proposing some  
14 modifications to equation 1. These modifications involved introducing several experimental  
15 parameters as presented by equation 2.<sup>16</sup>

$$\text{SSEF} = \frac{I_{\text{SERS}} \cdot (c_{\text{RS}} H_{\text{eff}})}{I_{\text{RS}} \cdot (\mu_{\text{M}} \mu_{\text{S}} A_{\text{M}})} \quad (2)$$

16  
17 Here  $H_{\text{eff}}$  is the effective height of the scattering volume,  $\mu_{\text{M}}$  is the surface density of the  
18 individual nanostructures producing the enhancement,  $\mu_{\text{S}}$  is the surface density of the molecules  
19 on the surface, and  $A_{\text{M}}$  represents the surface area of the SERS substrate. Although the above  
20 equation is assumed to give rigorous estimation of SSEF, it is still very hard to experimentally  
21 estimate some of the involved parameters with precision. Further, the issue regarding the precise  
22 estimation of Raman cross-section of the probe molecule both in solution and on surface till  
23 persists in this method. Therefore, the aim of this paper is to present a simplified and renewed  
24 approach for the experimental quantification of SSEF with improved precision.

## 2. Experimental Section

### 2.1. Chemicals and Materials

3-nitrophthalonitrile, cobalt (II) chloride, 1,8-diazabicyclo[5.4.0]-undec-7-ene and hydrogen tetrachloroaurate(III) hydrate were purchased from Sigma-Aldrich. All other chemicals used were of Analytical grade. The chemicals were used without any further purification. Polishing slurries and pads (Microcloth®) were purchased from Buehler, Germany. The diamond polished glassy carbon (GC) discs having a geometric of diameter  $0.785 \text{ cm}^2$  (HTW, Germany), polycrystalline gold discs (Au) having a geometric area of  $0.502 \text{ cm}^2$  (Mennica Metale Szlachetne, Warsaw, Poland) and indium tin oxide (ITO) coated glass slides (Sigma Aldrich) having a geometric area of  $0.250 \text{ cm}^2$  ( $0.5 \times 0.5 \text{ cm}$ ) were used as working electrodes. A platinum wire (Mennica Metale Szlachetne, Warsaw, Poland) was used as a counter electrode. Dry leakless electrode (DRIREF-2, World Precision Instruments, USA) was used as a reference electrode.

### 2.2. Instrumentation

All electrochemical experiments were carried out in a  $\mu$ Autolab potentiostat (Metrohm Autolab) with a custom-made three-electrode cell setup. All Raman measurements were performed using the Renishaw InVia Raman system equipped with 785 nm and 514 nm laser lines as excitation sources. The laser light was passed through a line filter and focused on a sample mounted on an X–Y–Z translation stage with a 50 $\times$  objective lens (numerical aperture 0.55) that focused the laser to a spot size of around 5  $\mu\text{m}$ . The Raman-scattered light was collected by the same objective through a holographic notch filter to block the Rayleigh scattering. A 1800 groove/ $\text{mm}^{-1}$  grating (514 nm source) and a 1200 groove/ $\text{mm}^{-1}$  grating (785

1  
2  
3 nm source) were used to provide a spectral resolution of  $5 \text{ cm}^{-1}$ . The Raman scattering signal  
4  
5 was recorded by a  $1024 \times 256$  pixel RenCam CCD detector. Typically, the spectra were acquired  
6  
7 for 4 s, with the laser power measured at the sample ranging from 1 mW to 50 mW. SERS  
8  
9 mapping was performed over all the substrates investigated and each spectrum presented here is  
10  
11 the average of 50 spectra. SEM measurements were performed using FEI Nova™ NanoSEM  
12  
13 Scanning Electron Microscope 450 with an accelerating voltage of 2 kV under high vacuum.  
14  
15  
16

### 17 18 19 *2.3. Synthesis of 1,8,15,22-Tetraaminophthalocyanatocobalt(II)*

20  
21 1,8,15,22-Tetraaminophthalocyanatocobalt(II) ( $4\alpha\text{-Co}^{\text{II}}\text{TAPc}$ ) (Scheme S1) was  
22  
23 synthesized based on the reported procedure.<sup>19, 20</sup> 3-nitrophthalonitrile (2.0 g, 11.6 mmol), cobalt  
24  
25 (II) chloride (0.83 g, 3.5 mmol) and catalytic amount of 1,8-diazabicyclo[5.4.0]-undec-7-ene  
26  
27 (DBU) were mixed together in a refluxing flask along with 100 mL of n-pentanol and refluxed  
28  
29 for 12h. The product was washed and centrifuged with methanol/water solution (v/v, 1/1) for 3  
30  
31 times to get a pure 1,8,15,22-tetranitrophthalocyanatocobalt(II). Then it was suspended in water  
32  
33 (150 mL) along with sodium sulfide (8 g) and stirred for 7 h at  $50^\circ\text{C}$ . The solid product obtained  
34  
35 after filtration was washed with dilute HCl and water. The product was again washed with water  
36  
37 and methanol each 3 times and dried.  
38  
39  
40  
41  
42

### 43 44 *2.4. SERS Substrate Preparation*

45  
46 GC and Au disc electrodes were mechanically mirror-polished with alumina slurries with  
47  
48 sequentially decreasing particle sizes ( $0.5 \mu\text{m}$ ,  $0.05 \mu\text{m}$  and  $0.02 \mu\text{m}$ ). After each step of  
49  
50 polishing, the electrodes were immersed in Millipore water and subsequently sonicated in an  
51  
52 aqueous ultrasonic bath for 15 minutes to remove the physically adsorbed alumina particles from  
53  
54 the electrode surface. The ITO coated glass slides were cleaned by sonicating in acetone  
55  
56  
57  
58  
59  
60

1  
2  
3 followed by ethanol for 15 minutes each. All the electrodes were finally washed with Millipore  
4  
5 water and dried with a flow of argon gas.  
6  
7

8 Nanostructured SERS substrate was prepared by potentiostatic deposition of gold over  
9  
10 GC (GC/Au), Au (pAu/Au) and ITO (ITO/Au). The three-electrode electrochemical cell was  
11  
12 filled with the solution of 4 mM HAuCl<sub>4</sub> in 0.1 M HClO<sub>4</sub> and subsequently purged with argon  
13  
14 gas for 30 min to remove most of the air from the solution. A potential of -80 mV was applied  
15  
16 for 400 s and then the electrode was removed from the solution and subsequently washed with  
17  
18 Millipore water to remove other ions from the surface. The electrode was then dried with flow of  
19  
20 Millipore water to remove other ions from the surface. The electrode was then dried with flow of  
21  
22 argon gas and used as a SERS substrate.  
23  
24

### 25 *2.5. Self-assembly of Tetraaminophthalocyanatocobalt(II) on Au Surfaces*

26  
27

28 The real surface area of GC/Au, pAu, pAu/Au, ITO/Au were estimated from the charge  
29  
30 required to reduce the surface gold oxide layer.<sup>21</sup> The geometric area of the GC (10 mm) and Au  
31  
32 (8 mm) electrodes were calculated using the diameter of the employed electrodes. The ratio of  
33  
34 the real surface area to the geometric area represents the surface roughness factor. The self-  
35  
36 assembled monomolecular film (SAM) of 4 $\alpha$ -Co<sup>II</sup>TAPc was formed by soaking the cleaned GC  
37  
38 and GC/Au electrode in 1 mM DMF solution of 4 $\alpha$ -Co<sup>II</sup>TAPc overnight. The electrode was then  
39  
40 removed from the solution and repeatedly washed with DMF and then dipped in DMF for 30 min  
41  
42 to remove physically adsorbed molecules from the electrode surface and finally washed with  
43  
44 water. The charge under the anodic wave corresponding to the oxidation of Co(II) was used to  
45  
46 calculate the surface coverage ( $\Gamma$ ). Fig. S1 shows the UV-visible spectrum of 4 $\alpha$ -Co<sup>II</sup>TAPc  
47  
48 SAM on ITO surface.  
49  
50  
51  
52  
53  
54  
55  
56  
57  
58  
59  
60

## 2.6. RRS and SERRS experiments

In order to reduce the error in quantification of SSEF, the same substrates were used for RRS/SERRS and cyclic voltammetry experiments. In addition, RRS/SERRS experiments were performed first then followed by cyclic voltammetry so that the effect of electrochemical reaction on the orientation of the molecule and hence the Raman signal is excluded.

## 3. Results and Discussion

### 3.1. Overview of Renewed Approach

Previously, Hildebrandt and Stockburger demonstrated an approach and a mathematical equation for the quantification of SSEF.<sup>22</sup> We recently employed the equation given by Hildebrandt et.al<sup>22</sup> for the quantification of SSEF for silver colloids.<sup>22-25</sup> The modified form of that equation is:

$$\text{SSEF} = \frac{I_{\text{SERRS}} \cdot c_{\text{RRS}}}{I_{\text{RRS}} \cdot c_{\text{SERRS}}} \quad (3)$$

Here,  $c_{\text{RRS}}$  and  $c_{\text{SERRS}}$  are the concentrations of molecules involved in resonance Raman scattering (RRS) and surface-enhanced resonance Raman scattering (SERRS), respectively. The parameter shielding constant ( $k$ ) is removed from the original equation.<sup>22</sup> Since the SERRS experiments in the present work has been carried out on solid substrate with a monolayer of probe molecule, the possibility of shielding effect contribution is negligible.

The principle of our approach to estimate the SSEF is based on deducting the RRS effect from SERRS. To achieve this demonstrating both RRS and SERRS in solid surfaces modified with a monolayer of electro- and Raman-active probe molecule is very crucial. In addition, for

1  
2  
3 the success of this approach, all important parameters such as Raman cross-section, focal volume  
4 and laser power must remain the same in both the RRS and SERRS experiments. By measuring  
5  
6 both the RRS (plasmon inactive) and SERRS (plasmon active) on surfaces having a monolayer  
7  
8 of electro- and Raman-active probe molecule, we can avoid the quantification of parameters such  
9  
10 as focal volume, solvent effect, shielding effect and inner filter effect. The compound which  
11  
12 satisfies our needs to quantify SSEF based on renewed approach is 1,8,15,22-  
13  
14 tetraaminophthalocyanatocobalt(II) ( $4\alpha\text{-Co}^{\text{II}}\text{TAPc}$ ). It forms a very stable monomolecular film  
15  
16 on GC,<sup>26</sup> Au,<sup>27, 28</sup> Ag<sup>27</sup> and indium tin oxide (ITO)<sup>29</sup> surfaces.  $4\alpha\text{-Co}^{\text{II}}\text{TAPc}$  is a very good  
17  
18 electro-active molecule which demonstrates well-defined redox peak for the  $\text{Co}^{\text{II}}/\text{Co}^{\text{III}}$  redox  
19  
20 couple.<sup>19, 28</sup> In addition,  $4\alpha\text{-Co}^{\text{II}}\text{TAPc}$  shows a very strong absorption band, known as Q band,  
21  
22 around 750 nm in the UV-visible spectroscopy.<sup>29</sup>  
23  
24  
25  
26  
27  
28  
29

30 Now comes the issue of Raman cross-section, a critical point which has to be addressed.  
31  
32 In fact, the key assumption in the present approach is that, identifying the Raman cross-section  
33  
34 of the probe molecule is not necessary (see section 4 for details) since in both of the RRS and  
35  
36 SERRS experiments, the chromophore ( $4\alpha\text{-Co}^{\text{II}}\text{TAPc}$ ) is in resonant condition. However,  
37  
38 estimating the parameters  $c_{\text{RRS}}$  and  $c_{\text{SERRS}}$  in equation 3 remains a challenge. Currently in all of  
39  
40 the existing methods,  $c_{\text{RRS}}$  and  $c_{\text{SERRS}}$  cannot be accurately measured without making some  
41  
42 theoretical assumptions.<sup>14, 16</sup> Nevertheless, based on our renewed approach, the above two  
43  
44 parameters can be rigorously quantified by preparing a self-assembled monolayer (SAM) of an  
45  
46 electrochemically redox-active chromophore molecule. In the present method, we developed a  
47  
48 monolayer of  $4\alpha\text{-Co}^{\text{II}}\text{TAPc}$  on a plasmon inactive glassy carbon (GC) and plasmon active  
49  
50 nanostructure gold over GC (GC/Au) surfaces/electrodes such that both the surfaces are suitable  
51  
52 for electrochemical and Raman (RRS and SERRS) experiments. By integrating the charge under  
53  
54  
55  
56  
57  
58  
59  
60

1  
2  
3 the redox wave of the cyclic voltammograms obtained for  $4\alpha\text{-Co}^{\text{II}}\text{TAPc}$ , the surface coverage  
4  
5 i.e.,  $c_{\text{RRS}}$  and  $c_{\text{SERRS}}$  can be accurately estimated (vide infra). Now, equation 3 can be rearranged  
6  
7  
8 as:

$$\text{SSEF} = \frac{I_{\text{SERRS}} \cdot \Gamma_{\text{RRS}}}{I_{\text{RRS}} \cdot \Gamma_{\text{SERRS}}} \quad (4)$$

9  
10  
11  
12  
13  
14  
15  
16 Where,  $\Gamma_{\text{RRS}}$  and  $\Gamma_{\text{SERRS}}$  are the surface coverage of probe molecule on GC and GC/Au surfaces,  
17  
18 respectively. Here on GC surface, selecting an excitation laser line which is in resonance with  
19  
20 the chromophore leads to RRS enhancement only since the SERS effect is completely excluded  
21  
22 on the GC surface. On the other hand, on GC/Au surface, the chromophore experiences both  
23  
24 RRS and SERRS phenomenon. Since the exact surface coverage of  $4\alpha\text{-Co}^{\text{II}}\text{TAPc}$  on both RRS  
25  
26 and SERRS active surfaces are known and also other parameters such as laser power, focal area  
27  
28 and Raman cross-section remains same for both the experiments, the equation 4 is expected to  
29  
30 provide a SSEF value with improved accuracy than the earlier methods.  
31  
32  
33  
34

35  
36 We elected the compound 1,8,15,22-tetraaminophthalocyanatocobalt(II) ( $4\alpha\text{-Co}^{\text{II}}\text{TAPc}$ )  
37  
38 as it satisfies the sought criteria for the chromophore in our experiments. It is a very good redox-  
39  
40 active molecule with strong absorption band around 750 nm (Scheme S1). Moreover, it forms a  
41  
42 stable monomolecular film on GC, Au, Ag and indium tin oxide (ITO).<sup>26, 28, 29</sup>  
43  
44  
45

### 46 *3.2. Preparation, characterization and estimation of real surface area of the SERS substrates*

47  
48  
49 The SERS substrate used in the present investigation was prepared by potentiostatic  
50  
51 deposition of nanostructured Au over mirror polished GC surface/electrode. Here Au has been  
52  
53 preferred over traditionally used silver surface due to several reasons such as: (i) the wide  
54  
55 potential window of Au which makes the surface appropriate for  $4\alpha\text{-Co}^{\text{II}}\text{TAPc}$  redox couple; (ii)

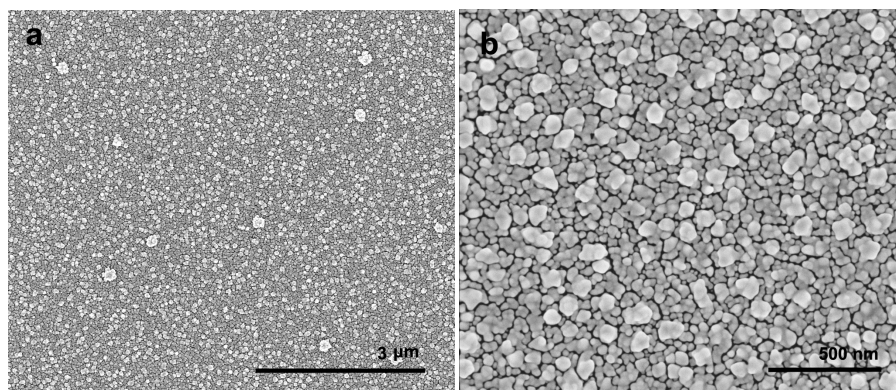


**Fig. 1** SEM images of nanostructured Au electrodeposited over mirror polished GC.

the ability to precisely estimate the real surface by electrochemical methods; (iii) the plasmonic band of nanostructured Au is red-shifted in contrast to rough silver, which will result in an increased SERS effect with red excitation line, and (iv) stability of the Au surface in open air. The surface morphology of GC/Au substrate was characterized by scanning electron microscopy (SEM) experiments (Fig. 1). The SEM picture clearly reveals a defect-free uniform deposition of Au nanostructures in the size ranging from 10 to 100 nm. The ellipsometry experiment depicts that the absorption maximum of the GC/Au substrate is around 500 nm (Fig. S2).

It is well established in the literature<sup>21, 30</sup> that real surface area of gold could be achieved electrochemically by integrating the charge under the gold oxide reduction peak. In the present study, a similar electrochemical approach has been followed to quantify the real surface area of GC/Au SERRS substrate.<sup>24,25</sup> Further, we used diamond polished GC surfaces in all our experiments since they have the very flat surface with negligible surface roughness. Therefore, in the case of diamond polished GC, the geometric area and real surface area are almost similar. However, it is important to note that the real surface of SERS-active substrate is not equivalent to its geometric surface since a SERS-active substrate is always highly roughened. In most of the

earlier SSEF calculation methods, the difference between the real and geometric areas was not clearly accounted.

The real surface area of Au nanostructure over GC surface has been precisely quantified through cyclic voltammetry (Fig. S3).<sup>21</sup> By integrating the charge under the gold oxide reduction peak, the real surface of Au was found to be 3.02 cm<sup>2</sup> which is 3.98 times higher than the geometric surface area (0.785 cm<sup>2</sup>).<sup>21</sup> As diamond polished GC is known for its highly polished surface, the surface roughness is almost negligible in the case of GC surface.

### 3.3. Estimation of surface coverage of 4 $\alpha$ -Co<sup>II</sup>TAPc on both GC and GC/Au surfaces

The ability of 4 $\alpha$ -Co<sup>II</sup>TAPc to form monomolecular film on GC and GC/Au surfaces, via chemisorptions, and subsequent precise quantification of its surface coverage by cyclic voltammetry method is well documented in the literature.<sup>26, 28, 29</sup> Since the real surface area of both the surfaces (GC and GC/Au) has now been identified (see section 3.2), the surface coverage of the 4 $\alpha$ -Co<sup>II</sup>TAPc monomolecular film on GC ( $\Gamma_{\text{RRS}}$ ) and GC/Au ( $\Gamma_{\text{SERRS}}$ ) surfaces

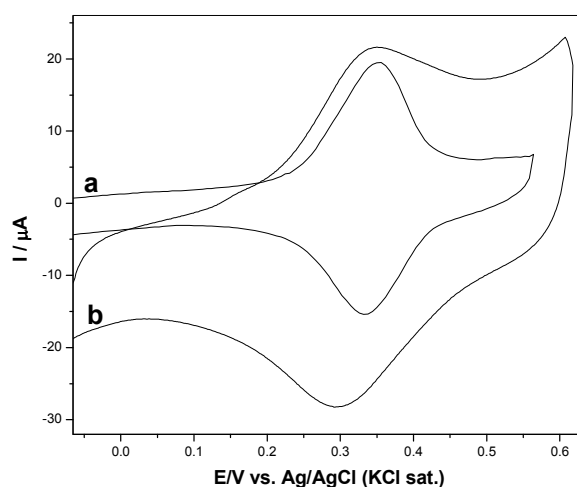


**Fig. 2** Cyclic voltammograms obtained for self-assembled monomolecular films of 4 $\alpha$ -Co<sup>II</sup>TAPc on (a) GC and (b) GC/Au electrodes in 0.1 M H<sub>2</sub>SO<sub>4</sub> at a scan rate of 0.1 Vs<sup>-1</sup>.

1  
2  
3 can also be quantified by integrating the charge under redox waves of the obtained cyclic  
4 voltammogram in Fig. 2. The cyclic voltammograms (CVs) of GC/4 $\alpha$ -Co<sup>II</sup>TAPc and GC/Au/4 $\alpha$ -  
5 Co<sup>II</sup>TAPc electrodes were performed in 0.1 H<sub>2</sub>SO<sub>4</sub> (Fig. 2). The CVs showed a pair of well-  
6 defined redox couple with an E<sub>1/2</sub> value around 0.34 V corresponding to Co<sup>III</sup>/Co<sup>II</sup> redox  
7 couple.<sup>19, 26</sup> The surface coverage ( $\Gamma$ ) of 4 $\alpha$ -Co<sup>II</sup>TAPc SAM on GC and on GC/Au electrodes has  
8 been estimated by integrating the charge under the anodic wave (Co<sup>II</sup> oxidation) of the cyclic  
9 voltammogram. The  $\Gamma$  values of  $2.25 \times 10^{-10}$  mol cm<sup>-2</sup> and  $8.61 \times 10^{-11}$  mol cm<sup>-2</sup> have been  
10 estimated for 4 $\alpha$ - Co<sup>II</sup>TAPc SAM on GC and on GC/Au surfaces/electrodes respectively. The  
11 values are in good agreement with the reported values.<sup>26</sup> The increased surface coverage on  
12 glassy carbon electrode is attributed in part to the additional  $\pi$ -stacking effect of 4 $\alpha$ -Co<sup>II</sup>TAPc on  
13 glassy carbon surface.<sup>26</sup> On the other hand, contribution of  $\pi$ -stacking on gold surface is  
14 insignificant.

### 3.4. Quantification of SERS substrate enhancement factor (SSEF)

15  
16  
17  
18  
19  
20  
21  
22  
23  
24  
25  
26  
27  
28  
29  
30  
31  
32  
33  
34  
35  
36  
37  
38  
39  
40  
41  
42  
43  
44  
45  
46  
47  
48  
49  
50  
51  
52  
53  
54  
55  
56  
57  
58  
59  
60  
Fig. 3 shows the RRS and SERRS spectra of 4 $\alpha$ -Co<sup>II</sup>TAPc SAM on GC and GC/Au surfaces, respectively. Both RRS and SERRS spectra on all surfaces showed two intense bands at 1551 cm<sup>-1</sup> and 756 cm<sup>-1</sup> corresponding to macrocycle in-plane stretching and macrocycle deformation, respectively.<sup>27, 31, 32</sup> Moreover, RRS spectrum on the GC surface showed two intense bands at 1309 cm<sup>-1</sup> and 1606 cm<sup>-1</sup> corresponding to the stretching and breathing modes of sp<sup>2</sup> hybridized carbon.<sup>33</sup> To quantify the SSEF, the band at 756 cm<sup>-1</sup> is used as a reference. Based on equation 4, the SSEF of GC/Au surface has been calculated and it was found to be  $(2.82 \pm 0.22)10^4$ . It is worth to mention at this juncture that all the 50 SERRS spectra recorded at

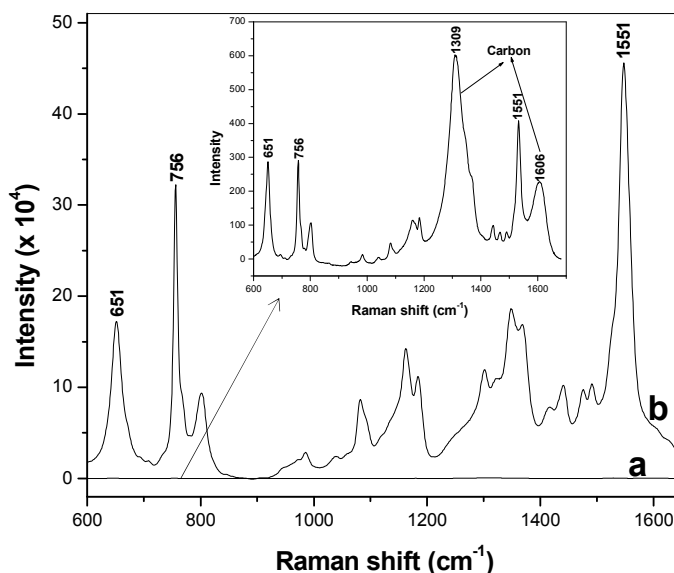


**Fig. 3** (a) RRS and (b) SERRS spectra of self-assembled monomolecular film of  $4\alpha\text{-Co}^{\text{II}}\text{TAPc}$  on GC and GC/Au surfaces. Inset shows the closer view of RRS spectrum.

different spots on the GC/Au surface have similar intensity ratio among the different stretching bands confirming that all the  $4\alpha\text{-Co}^{\text{II}}\text{TAPc}$  molecules adopt same orientation over the entire substrate. We have also carried out the Raman experiment of  $4\alpha\text{-Co}^{\text{II}}\text{TAPc}$  SAM on GC surface at non-resonance condition using 514 nm laser line as the excitation source. The absence of Raman bands corresponding to  $4\alpha\text{-Co}^{\text{II}}\text{TAPc}$  molecule even after increasing the laser accumulation to 10 times higher than that used for the RRS measurement with 785 nm laser line confirms that there is no charge-transfer enhancement on GC surface. This clearly implies that only resonance Raman effect contribute to the Raman spectrum of  $4\alpha\text{-Co}^{\text{II}}\text{TAPc}$  SAM on GC surface under red light excitation (785 nm). Further, it is worth to mention here that the overall estimated SSEF by the present method is the average value from whole surface and not at a particular spot. Therefore, the quantified SSEF by the present method is the average SSEF (ASSEF).

### 3.5. Quantification of SSEF of ITO/Au and pAu/Au substrates

In order to confirm that the present approach could be used for wide variety of surfaces, we have performed the same experiment on Au deposited on indium tin oxide (ITO/Au) and also on Au deposited over mirror polished Au surface (pAu/Au). Fig. 4 show the SEM pictures of ITO/Au and pAu/Au substrates and it clearly depicts that the Au nanostructures are uniformly deposited over the entire surface. Further, a closer look reveals that the size of Au nanostructures deposited over polished Au surface is smaller than those deposited over GC and ITO surfaces. The probable cause may be the particle initiation spots on Au surface are higher than the other surfaces due to better Au-Au interaction. Similar to GC/Au surface, the real surface area of nanostructured pAu/Au and ITO/Au was estimated from the gold oxide reduction peak (Fig. S4) and it was found to be  $2.33 \text{ cm}^2$  and  $4.84 \text{ cm}^2$ , respectively. The  $\Gamma$  values of  $4.96 \times 10^{-11} \text{ mol cm}^{-2}$  and  $1.27 \times 10^{-11} \text{ mol cm}^{-2}$  have been estimated for  $4\alpha\text{-Co}^{\text{II}}\text{TAPc}$  SAM on pAu/Au and ITO/Au surfaces/electrodes, respectively (Fig. S5).

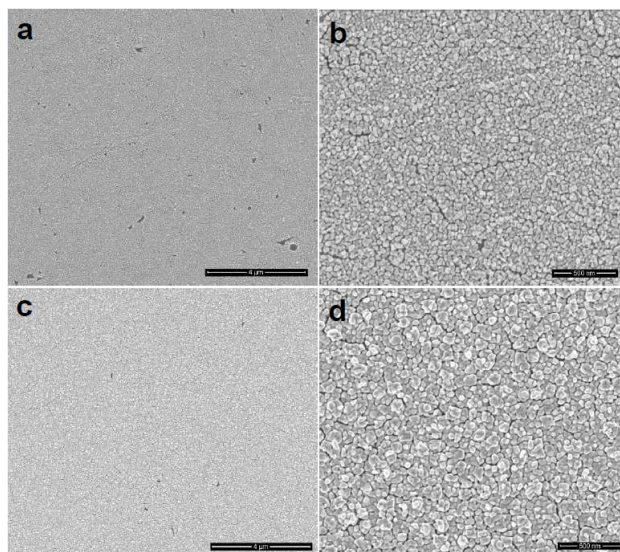


**Fig. 4** SEM images of nanostructured Au electrodeposited over polished Au (a, b) and ITO (c, d) substrates captured under different magnifications.

For the estimation of SSEF in all the three SERS substrate, RRS of  $4\alpha\text{-Co}^{\text{II}}\text{TAPc}$  performed on the GC surface has been used as common reference since one can be certain that GC is a plasmon-inactive surface and therefore it will not provide SERS enhancement. Fig. 5 shows the SERS spectra of  $4\alpha\text{-Co}^{\text{II}}\text{TAPc}$  on pAu/Au and ITO/Au substrates. The SSEF of ITO/Au and pAu/Au was quantified by substituting the above values in equation 4 and it was found to be  $(6.3 \pm 0.59)10^4$  and  $(2.1 \pm 0.19)10^5$ , respectively (nearly 1 order higher SSEF on pAu/Au than other two substrates). This may be attributed to the possible coupling between the propagating surface plasmon polariton (SPP) of the underlying polished Au surface and surface plasmon resonance (SPR) of the Au nanostructures i.e., SPP-SPR coupling.<sup>34</sup> In addition, the nanostructures on pAu has smaller grain size than on GC or ITO surfaces which allows the possibility for more ‘hot spots’ in the former surface and subsequent higher SSEF.

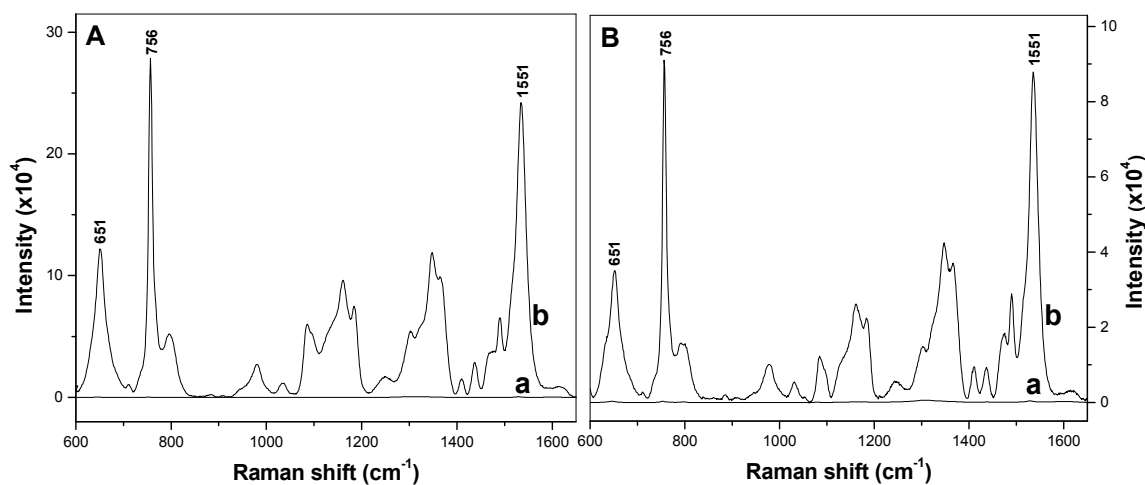


**Fig. 5** SERRS spectra of self-assembled monomolecular film of  $4\alpha\text{-Co}^{\text{II}}\text{TAPc}$  on pAu/Au (Aa) and ITO/Au (Ab) substrates. RRS spectrum of self-assembled monomolecular film of  $4\alpha\text{-Co}^{\text{II}}\text{TAPc}$  on GC (both Aa and Ba) which is the replicate of Fig. 3 inset.

### 3.6. Analyzing the SSEF values of the present method with traditional method

To have a comparative study, we have calculated the SSEF for our substrates in the traditional way of calculation i.e., using the parameters  $N_{\text{vol}}$  and  $N_{\text{Surf}}$ . The number of molecules in the surface,  $N_{\text{Surf}}$  is calculated by assuming a Langmuir monolayer.

As we discussed earlier, it is hard to accurately estimate the number of molecules in the solution medium that exists under the focus of laser beam. To have a better comparison, we considered three possible focal volumes such as cylindrical, fusi form and whole cell length for the estimation of  $N_{\text{vol}}$ . Table 1 indicates the SSEF values acquired using our method in comparison to those obtained by the traditional method.<sup>14, 16</sup> It can be observed from the table that the SSEF values calculated by the traditional method show significantly greater variations than those calculated using equation 4. These results indicate the improved precession in our approach when compared to the traditional approach.

**Table 1** Comparison of SSEF of the all the three substrates calculated by the present approach with the traditional method.

SERS substrate	Traditional way of SSEF calculation			Present method
	Cylindrical laser beam	Fusiform laser beam	Whole cell length	
GC/Au	$4.9 \times 10^3$	$1.6 \times 10^3$	$1.1 \times 10^6$	$2.8 \times 10^4$
pAu/Au	$2.1 \times 10^4$	$6.9 \times 10^3$	$4.6 \times 10^6$	$2.1 \times 10^5$
ITO/Au	$7.2 \times 10^3$	$2.4 \times 10^3$	$1.6 \times 10^6$	$6.3 \times 10^4$

## 4. Addressing critical issues

In spite of all the above explanation of the renewed approach, there are few issues and shortcomings in the above equation which has to be criticized and addressed. In our approach the

1  
2  
3 RRS effect of  $4\alpha\text{-Co}^{\text{II}}\text{TAPc}$  is assumed to be similar on both GC and GC/Au surfaces. This  
4  
5 assumption may not be completely valid since there will be some differences between the two  
6  
7 surface with respect to the RRS effect. This is due to the potential differences in the surface  
8  
9 binding nature of the  $4\alpha\text{-Co}^{\text{II}}\text{TAPc}$  molecules on each surface. Actually, RRS effect is directly  
10  
11 related to the Raman cross-section and since the present study involved the RRS and SERRS  
12  
13 measurements on surfaces having monomolecular  $4\alpha\text{-Co}^{\text{II}}\text{TAPc}$  film, the Raman cross-section  
14  
15 exclusively depends on the charge-transfer effect i.e. the chemical enhancement factor (CHEF).  
16  
17 In other words, the difference in surface binding nature of  $4\alpha\text{-Co}^{\text{II}}\text{TAPc}$  on GC and GC/Au  
18  
19 surface, more precisely the difference in chemical enhancement factor (CHEF), is playing key  
20  
21 role in our assumption rather than the molecular orientation of the chromophore on the surface. It  
22  
23 is well-known that the contribution of chemical enhancement factor (CHEF) to the overall SSEF  
24  
25 is small even for organothiols on noble metal nanoparticles.<sup>11</sup> Considering the fact that the  
26  
27 binding affinity of amino groups on GC or Au are comparatively weaker than the binding  
28  
29 affinity of thiols on gold surface, the contribution of CHEF in the present study is assumed to be  
30  
31 even less than the values indicated in the literature for organothiol-noble metal interaction.<sup>11</sup>  
32  
33 Overall, in the present method, it is only the ratio between the CHEF of chromophore on the GC  
34  
35 and GC/Au surfaces contributing to the overall SSEF and we believe this will be an insignificant  
36  
37 number. Further, a recent report<sup>35</sup> demonstrated that the chemical effect hardly influences the  
38  
39 resonance Raman effect in particular for larger molecules such as Rhodamine 6G which further  
40  
41 supports our assumption. Therefore, we believe that the difference in the RRS effect i.e., charge-  
42  
43 transfer effect of  $4\alpha\text{-Co}^{\text{II}}\text{TAPc}$  on both surfaces is negligible.  
44  
45  
46  
47  
48  
49  
50  
51  
52

53 The other major concern for the readers would be the feasibility of the present approach  
54  
55 to quantify SSEF for the non-conducting surface. In principle, the methodology could be  
56  
57

60

1  
2  
3 extended to non-conductive surface. The real surface area of any nanostructure surface could be  
4  
5 precisely estimated by Brunauer–Emmett–Teller (BET) gas adsorption method<sup>36</sup> and  
6  
7 subsequently one can relatively estimate the number of  $4\alpha\text{-Co}^{\text{II}}\text{TAPc}$  on any Au nanostructured  
8  
9 surface by using the standard surface coverage value of  $4\alpha\text{-Co}^{\text{II}}\text{TAPc}$  on Au surface ( $8.61 \times 10^{-11}$   
10  
11  $\text{mol cm}^{-2}$ ) estimated electrochemically.<sup>28</sup> Since surface coverage of  $4\alpha\text{-Co}^{\text{II}}\text{TAPc}$  directly related  
12  
13 to gold surface area irrespective of the surface morphology of gold surface, we strongly believe  
14  
15 the above value ( $8.61 \times 10^{-11} \text{ mol cm}^{-2}$ ) is valid for any gold surface. As an evidence, the present  
16  
17 number is already going in hand with the literature.<sup>28</sup> Thus, by assessing the RRS and SERRS  
18  
19 intensity of  $4\alpha\text{-Co}^{\text{II}}\text{TAPc}$ , respectively on diamond polished GC and SERRS active Au surface  
20  
21 along with the real surface area (BET method) of SERRS active Au substrate, one can relatively  
22  
23 quantify the SSEF of a new Au surface by utilizing the surface coverage value of  $4\alpha\text{-Co}^{\text{II}}\text{TAPc}$   
24  
25 on GC and GC/Au surfaces from the present work as a standard value.  
26  
27  
28  
29  
30  
31

32  
33 The equation proposed in our study (equation 4), in the present form, may not be suitable  
34  
35 to quantify the SSEF from colloidal nanoparticles. This is because several other parameters must  
36  
37 be included in the equation. For example, the precise surface area of the nanoparticles, the  
38  
39 surface coverage by the probe molecule, contribution of EF from second and subsequent layers  
40  
41 of the analyte on the nanoparticle surface, the shielding and inner filter effect of the nanoparticles  
42  
43 will be required for the quantification of SSEF.  
44  
45  
46

## 47 **5. Conclusions**

48  
49  
50 In summary, we have derived a most simplified equation, of improved precision, for the  
51  
52 quantification of SSEF by a renewed approach. This approach uses electroactive and SERRS  
53  
54 active  $4\alpha\text{-Co}^{\text{II}}\text{TAPc}$  as a probe molecule. The SSEF from the GC/Au, pAu/Au and ITO/Au  
55  
56  
57  
58  
59  
60

1  
2  
3 SERS substrates has been quantified using  $4\alpha\text{-Co}^{\text{II}}\text{TAPc}$  as a standard molecule for red light  
4  
5 excitation. The number of  $4\alpha\text{-Co}^{\text{II}}\text{TAPc}$  molecules involved in RRS and SERRS have been  
6  
7 precisely quantified by electrochemical experiments.  
8  
9

10  
11 Our approach relies on performing RRS on Plasmon-inactive conductive surface and  
12  
13 subsequently deducting RRS from SERRS to end up with surface enhancement. This approach is  
14  
15 also based on the assumption that the resonance enhancement in the Raman spectra is surface-  
16  
17 independent. It is important to note that, the SSEF of a substrate is related to the excitation laser  
18  
19 used since each surface has its own surface plasmon resonance frequency. Thus, the calculated  
20  
21 SSEF for all three substrates is applicable only for 785 nm laser line. The present approach for  
22  
23 SSEF quantification can be extended to the quantification of SSEF from various conducting and  
24  
25 non-conducting SERS substrates at various excitation wavelengths provided redox-active Raman  
26  
27 chromophores suitable for each laser line. We are presently working towards the quantification  
28  
29 of SSEF from silver surface using a substituted porphyrin and also BET method to estimate the  
30  
31 real surface area. This chromophore is electroactive and resonance Raman active at 413 nm  
32  
33 excitation line and, therefore, satisfies the requirements of our proposed approach.  
34  
35  
36  
37  
38  
39

#### 40 **Acknowledgments**

41  
42  
43 The research was supported by the Foundation for Polish Science - POMOST Programme  
44  
45 co-financed by the European Union within European Regional Development Fund. AS was  
46  
47 supported by the EC 7.FP under the Research Potential (Coordination and Support Actions FP7-  
48  
49 REGPOT-CT-2011-285949-NOBLESSE). R.H. was supported by the National Science Center in  
50  
51 the project from the funds granted on the basis of the decision number: DEC-  
52  
53 2013/08/W/NZ1/00687 (SYMFONIA). AS sincerely thank Prof. Godwin Ayoko, Dr. Bill Lott,  
54  
55  
56

1  
2  
3 Prof. Peter Fredericks, Prof. Esa Jaatinen and Dr. Llew Rintoul from QUT for their valuable  
4  
5 discussion and support.  
6  
7

## 8 9 References

- 10 1. M. Fleischmann, P. Hendra and A. McQuillan, *Chemical Physics Letters*, 1974, **26**, 163-166.
- 11 2. A. Sivanesan, E. Witkowska, W. Adamkiewicz, Ł. Dziewit, A. Kamińska and J. Waluk, *Analyst*,  
12 2014, **139**, 1037-1043.
- 13 3. S.-C. Luo, K. Sivashanmugan, J.-D. Liao, C.-K. Yao and H.-C. Peng, *Biosensors and Bioelectronics*,  
14 2014, **61**, 232-240.
- 15 4. S. S. R. Dasary, A. K. Singh, D. Senapati, H. Yu and P. C. Ray, *Journal of the American Chemical*  
16 *Society*, 2009, **131**, 13806-13812.
- 17 5. W. Ren, Y. Fang and E. Wang, *ACS Nano*, 2011, **5**, 6425-6433.
- 18 6. E.-Z. Tan, P.-G. Yin, T.-t. You, H. Wang and L. Guo, *ACS Applied Materials & Interfaces*, 2012, **4**,  
19 3432-3437.
- 20 7. S. Nie and S. R. Emory, *science*, 1997, **275**, 1102-1106.
- 21 8. K. Kneipp, Y. Wang, H. Kneipp, L. T. Perelman, I. Itzkan, R. R. Dasari and M. S. Feld, *Physical*  
22 *Review Letters*, 1997, **78**, 1667.
- 23 9. M. Muniz-Miranda and G. Sbrana, *The Journal of Physical Chemistry B*, 1999, **103**, 10639-10643.
- 24 10. S. M. Ansar, X. Li, S. Zou and D. Zhang, *The Journal of Physical Chemistry Letters*, 2012, **3**, 560-  
25 565.
- 26 11. F. S. Ameer, W. Hu, S. M. Ansar, K. Siriwardana, W. E. Collier, S. Zou and D. Zhang, *The Journal of*  
27 *Physical Chemistry C*, 2013, **117**, 3483-3488.
- 28 12. W. B. Cai, B. Ren, X. Q. Li, C. X. She, F. M. Liu, X. W. Cai and Z. Q. Tian, *Surface Science*, 1998, **406**,  
29 9-22.
- 30 13. A. D. McFarland, M. A. Young, J. A. Dieringer and R. P. Van Duyne, *The Journal of Physical*  
31 *Chemistry B*, 2005, **109**, 11279-11285.
- 32 14. E. C. Le Ru and P. G. Etchegoin, *MRS Bulletin*, 2013, **38**, 631-640.
- 33 15. M. J. Natan, *Faraday Discussions*, 2006, **132**, 321-328.
- 34 16. E. C. Le Ru, E. Blackie, M. Meyer and P. G. Etchegoin, *The Journal of Physical Chemistry C*, 2007,  
35 **111**, 13794-13803.
- 36 17. L. Jensen and G. C. Schatz, *The Journal of Physical Chemistry A*, 2006, **110**, 5973-5977.
- 37 18. S. A. Meyer, E. C. L. Ru and P. G. Etchegoin, *The Journal of Physical Chemistry A*, 2010, **114**, 5515-  
38 5519.
- 39 19. A. Sivanesan and S. Abraham John, *Electrochimica Acta*, 2008, **53**, 6629-6635.
- 40 20. A. Sivanesan and S. A. John, *Biosensors and Bioelectronics*, 2007, **23**, 708-713.
- 41 21. J. C. Hoogvliet, M. Dijkstra, B. Kamp and W. P. Van Bennekom, *Analytical Chemistry*, 2000, **72**,  
42 2016-2021.
- 43 22. P. Hildebrandt and M. Stockburger, *The Journal of Physical Chemistry*, 1984, **88**, 5935-5944.
- 44 23. A. Sivanesan, H. K. Ly, J. Kozuch, M. Sezer, U. Kuhlmann, A. Fischer and I. M. Weidinger,  
45 *Chemical Communications*, 2011, **47**, 3553-3555.
- 46 24. G. Kalaivani, A. Sivanesan, A. Kannan, N. S. Venkata Narayanan, A. Kaminska and R. Sevvell,  
47 *Langmuir*, 2012, **28**, 14357-14363.
- 48 25. A. Sivanesan, J. Kozuch, H. K. Ly, G. Kalaivani, A. Fischer and I. M. Weidinger, *RSC Advances*,  
49 2012, **2**, 805-808.

- 1
  - 2
  - 3
  - 4
  - 5
  - 6
  - 7
  - 8
  - 9
  - 10
  - 11
  - 12
  - 13
  - 14
  - 15
  - 16
  - 17
  - 18
  - 19
  - 20
  - 21
  - 22
  - 23
  - 24
  - 25
  - 26
  - 27
  - 28
  - 29
  - 30
  - 31
  - 32
  - 33
  - 34
  - 35
  - 36
  - 37
  - 38
  - 39
  - 40
  - 41
  - 42
  - 43
  - 44
  - 45
  - 46
  - 47
  - 48
  - 49
  - 50
  - 51
  - 52
  - 53
  - 54
  - 55
  - 56
  - 57
  - 58
  - 59
  - 60
26. A. Sivanesan and S. A. John, *Electrochimica Acta*, 2009, **54**, 7458-7463.
27. M. P. Somashekarappa and S. Sampath, *Chemical Communications*, 2002, **0**, 1262-1263.
28. A. Sivanesan and S. Abraham John, *Langmuir*, 2008, **24**, 2186-2190.
29. A. Sivanesan and S. Abraham John, *Journal of Electroanalytical Chemistry*, 2009, **634**, 64-67.
30. S. Trasatti and O. A. Petrii, *Journal of Electroanalytical Chemistry*, 1992, **327**, 353-376.
31. C. Jennings, R. Aroca, A.-M. Hor and R. O. Loutfy, *Journal of Raman Spectroscopy*, 1984, **15**, 34-37.
32. X. Li, W. Xu, X. Wang, H. Jia, B. Zhao, B. Li and Y. Ozaki, *Thin Solid Films*, 2004, **457**, 372-380.
33. D. R. Tallant, J. E. Parmeter, M. P. Siegal and R. L. Simpson, *Diamond and Related Materials*, 1995, **4**, 191-199.
34. N. Félidj, J. Aubard, G. Lévi, J. R. Krenn, G. Schider, A. Leitner and F. R. Aussenegg, *Physical Review B*, 2002, **66**, 245407.
35. K.-i. Yoshida, T. Itoh, H. Tamaru, V. Biju, M. Ishikawa and Y. Ozaki, *Physical Review B*, 2010, **81**, 115406.
36. Y. H. Tan, J. A. Davis, K. Fujikawa, N. V. Ganesh, A. V. Demchenko and K. J. Stine, *Journal of Materials Chemistry*, 2012, **22**, 6733-6745.